Landscape Ecol (2018) 33:2253–2272
https://doi.org/10.1007/s10980-018-0739-4

RESEARCH ARTICLE

Physical drivers of seagrass spatial configuration: the role of thresholds

Amy V. Uhrin · Monica G. Turner

Received: 24 June 2018 / Accepted: 30 October 2018 / Published online: 13 November 2018

Abstract
Context Seagrass landscapes vary substantially in extent and pattern, resulting from depth zonation and hydrodynamic stress gradients and may exhibit threshold behavior in response to changes in physical drivers. Seagrass landscapes persist in a delicate balance between processes of disturbance and recovery and therefore may exhibit behavior typical of classic critical systems.
Objectives Examine how hydrodynamic drivers and physical setting influence seagrass landscape composition and configuration. Determine if seagrass patch size distributions typify patterns observed for critical systems.
Methods We used landscape metrics to quantify the spatial configuration of seagrass and then modeled the response of these metrics to wave energy, tidal current speed, and water depth at 62 estuarine sites in North Carolina, USA. Seagrass landscapes were representative of cover types observed in the estuary generated by wave energy.
Results Percent cover, patch size, and number of patches all declined with increasing wave energy. Threshold behavior occurred at wave energy change points between 675–774 J m^{-1}. Seagrass landscapes differed in spatial configuration and physical setting, above and below change points. There was moderate support for a power law relationship for patch size distribution across a wide range of seagrass landscape cover and wave energy.
Conclusions With weather extremes on the rise, much of this estuarine seagrass will be exposed to increased wave energy. Where seagrass exists just below the wave energy change points, increases in wave energy could tip those habitats into a new stable state of lower cover resulting in less cover overall in the estuary.

Keywords Seagrass · Spatial configuration · Hydrodynamics · Ecological thresholds · Alternate state · North Carolina

Electronic supplementary material The online version of this article (https://doi.org/10.1007/s10980-018-0739-4) contains supplementary material, which is available to authorized users.

A. V. Uhrin (✉)
Marine Debris Division, Department of Commerce, National Oceanic and Atmospheric Administration, National Ocean Service, Office of Response and Restoration, 1305 East West Highway, SSMC4, Room10240, Silver Spring, MD, USA
e-mail: amy.uhrin@noaa.gov

M. G. Turner
Department of Integrative Biology, University of Wisconsin, 430 Lincoln Drive, Madison, WI 53706, USA

Introduction

Ecological systems that experience well-mixed disturbances (the disturbance agent is fast or large compared to recovery processes) may exhibit classical critical behavior where local processes of disturbance and recovery lead to the emergence of large-scale spatial pattern (Pascual and Guichard 2005). Classical critical systems may exhibit threshold behavior where slight changes in environmental drivers produce abrupt responses in ecosystem qualities and properties (Groffman et al. 2006) often leading to a state (phase) transition at the critical point, or threshold (Scheffer and Carpenter 2003; Solé 2011; Kéfi et al. 2014). Near such thresholds, spatial pattern emerges in which the statistical distribution of organisms exhibits scale invariance, i.e., the absence of an emergent, or defining spatial scale. In critical systems, the frequency distribution of cluster (patch) sizes of organisms comprising the landscape exhibits power law behavior where all patch sizes are present with no dominant size (Solé 2011). Thus, a scale-invariant distribution of organisms (e.g., vegetation cover) may suggest that the system is approaching a critical point of landscape cover and pattern change, and this type of spatial pattern could serve as an indicator of a system on the verge of transition to an alternate state (Rietkerk et al. 2004; Kéfi et al. 2007).

Understanding the relative importance of drivers of landscape pattern and whether landscape pattern exhibits threshold behavior in response to drivers remain key challenges in landscape ecology (Turner and Gardner 2015). Threshold behavior is likely specific to each driver-response combination, and a number of statistical methods exist for identifying thresholds or change points (that is, the value or restricted range of values of the controlling driver at which point substantial ecosystem change is observed; Qian et al. 2003; Toms and Lesperance 2003; Guénette and Villard 2004, 2005; Qian and Cuffney 2012). Change point identification has important resource management implications as it provides a quantitative reference point or decision criteria that prompts management action (Suding and Hobbs 2009; Samhouri et al. 2011) and can serve as a forewarning indicator of impending change (Sasaki et al. 2015).

It is possible that classical criticality underpins landscape cover and pattern in seagrass systems. Seagrass landscapes vary substantially in extent and pattern, and they persist given a delicate balance between processes of disturbance and recovery (den Hartog 1971; Fonseca et al. 1983). The spatial heterogeneity in seagrass landscapes results from depth zonation and localized hydrodynamic stress gradients (i.e., wind-wave exposure, tidal currents). The development of seagrass landscapes is tightly coupled with light availability, which decreases with water depth (Dennison et al. 1993). Most estuarine seagrass landscapes occur in shallow waters (e.g. 1–3 m) rather than deeper, light-limited waters, a result of water column turbidity from terrestrial runoff. A large, contiguous (one patch) seagrass meadow can develop in the absence of disturbance and in locations where current velocity, wave action, or biological disturbance (e.g., burrowing, grazing) are relatively low. Where current velocity and wave action are low but biological disturbance is high, a contiguous meadow may develop but with small gaps of bare sediment interspersed (Suchanek 1983; Valentine and Heck 1991; Christianen et al. 2014). In contrast, numerous small seagrass patches characterize locations where disturbances are more frequent, or current velocity, wave action, and perhaps bioturbation are relatively high. In addition, seagrasses 'migrate' across the seascape in response to sedimentary processes including erosion and sediment accretion, leading to temporal pattern dynamics (Patriquin 1975; Ferguson et al. 1993; Marba and Duarte 1995; Ferguson and Korfmacher 1997; Robbins and Bell 2000; Fonseca et al. 2008). These patterns likely develop as a dynamic equilibrium among seagrass colonization and recovery capabilities and the disturbance regime (den Hartog 1971; Patriquin 1975; Fonseca et al. 1983; Fonseca and Bell 1998; Koch et al. 2006; Walker et al. 2006).

Seagrass landscapes that exist at or near a hydrodynamic threshold or change point may be more susceptible to acute disturbances that can push the system beyond the threshold causing a state transition to one of less, or even no cover. Fonseca and Bell (1998) proposed threshold values for hydrodynamic drivers (wind-wave exposure and tidal current speed) and physical setting (water depth), above and below which noticeable differences in seagrass percent cover and perimeter to area ratio as well as sediment composition were observed. Following the passage of an extreme wind event, low percent cover seagrass landscapes consisting of small patches were observed

to experience higher seagrass loss via erosion at patch edges and complete loss of vegetative cover was observed in some cases (Fonseca and Bell 1998; Fonseca et al. 2000). Thus, the composition and spatial configuration of seagrass patches generated by physical drivers has implications for the maintenance of seagrass landscapes over time, particularly in response to acute disturbances like tropical cyclones (Fonseca and Bell 1998; Fonseca et al. 2000; Gera 2013; Gurbiscz et al. 2016). However, differences in seagrass spatial configuration across hydrodynamic gradients have not been well-described nor have thresholds in physical drivers been evaluated for the presence of telling, scale-invariant patterns. Seagrasses provide myriad ecosystem services including supporting (e.g., nutrient cycling, primary production), provisioning (e.g., marine life habitat, seafood), regulating (e.g., carbon sequestration, water quality), and cultural (e.g., recreation, economics), valued at $78–104 million USD per hectare depending on service type and valuation method (Dewsbury et al. 2016; Nordlund et al. 2016). Seagrasses are facing rapid declines worldwide (Orth et al. 2006; Waycott et al. 2009). Therefore, identifying thresholds in physical drivers and telling changes in landscape pattern in seagrass ecosystems is important because these can serve as forewarning indicators of impending change that may warrant management and conservation actions.

We studied two hydrodynamic drivers of seagrass landscape configuration (wave energy and tidal current speed) and one aspect of physical setting (water depth) in a lagoonal estuarine system with two codominant species. We analyzed effects of wave energy, tidal current speed, and water depth on seagrass landscape composition and configuration for seagrass landscapes of approximately 100 × 100 m. Specifically, we asked: (1) Which physical drivers most influence seagrass spatial pattern, (2) Do physical drivers exhibit threshold behavior where abrupt changes in seagrass pattern occur? (3) Is seagrass spatial pattern quantitatively different above and below physical driver thresholds? (4) Do seagrass landscapes exhibit scale-free pattern in patch size distributions?

Methods

Study area

The study was conducted in the Albemarle-Pamlico Sound Estuary System in North Carolina, the largest lagoonal estuarine system in the United States, bordered on the east and south by a chain of barrier islands (Outer Banks; Fig. 1). Exchange of seawater with the Atlantic Ocean occurs through eight active inlets that are highly dynamic and migratory. In addition to lunar tides, the system is characterized by variable and unpredictable wind-driven tides. Broad shallows, less than 2 m deep at mean lower low water, are punctuated by relatively few deeper basins and channels and feature fringing salt marshes and marsh islands, oyster reefs, and beds of seagrass. Near the mainland shoreline, fine silts and mud dominate the benthos (Kenworthy et al. 1982; Fonseca and Bell 1998), resulting in highly colored and turbid waters (reduced light penetration) which limits seagrasses to about 1.2 m depth (Biber et al. 2008). Moving away from the shoreline, sediments become more coarse (quartz sand; Kenworthy et al. 1982; Fonseca and Bell 1998), light penetration increases, and seagrasses can extend their depth limit to about 2 m (Ferguson and Korfmacher 1997; Biber et al. 2008). Seagrasses along this portion of the North Carolina coast cover an area of $\sim$ 554 km^2 behind the extensive barrier island system (APNEP 2012).

A mixture of two species co-dominate the system seasonally. The temperate *Zostera marina* (eelgrass) achieves peak biomass in winter to early summer while the tropical-subtropical *Halodule wrightii* (shoalgrass) attains highest biomass in late summer to early fall. Coastal North Carolina is the only known overlap in distribution of *Z. marina* and *H. wrightii* in the world (Thayer et al. 1984) with the Albemarle-Pamlico Sound Estuary System encompassing the greater part of this overlap. This overlapping distribution is very near the southern limit of *Z. marina* along the eastern seaboard of the United States and represents the northern limit of *H. wrightii*.

Seagrass landscape pattern in this system is largely the result of hydrodynamic forcing (Fonseca et al. 1983; Fonseca and Bell 1998; Fig. 2). Where current velocity and wave action are low, large, contiguous (one patch) seagrass meadows develop. In contrast, numerous small seagrass patches characterize

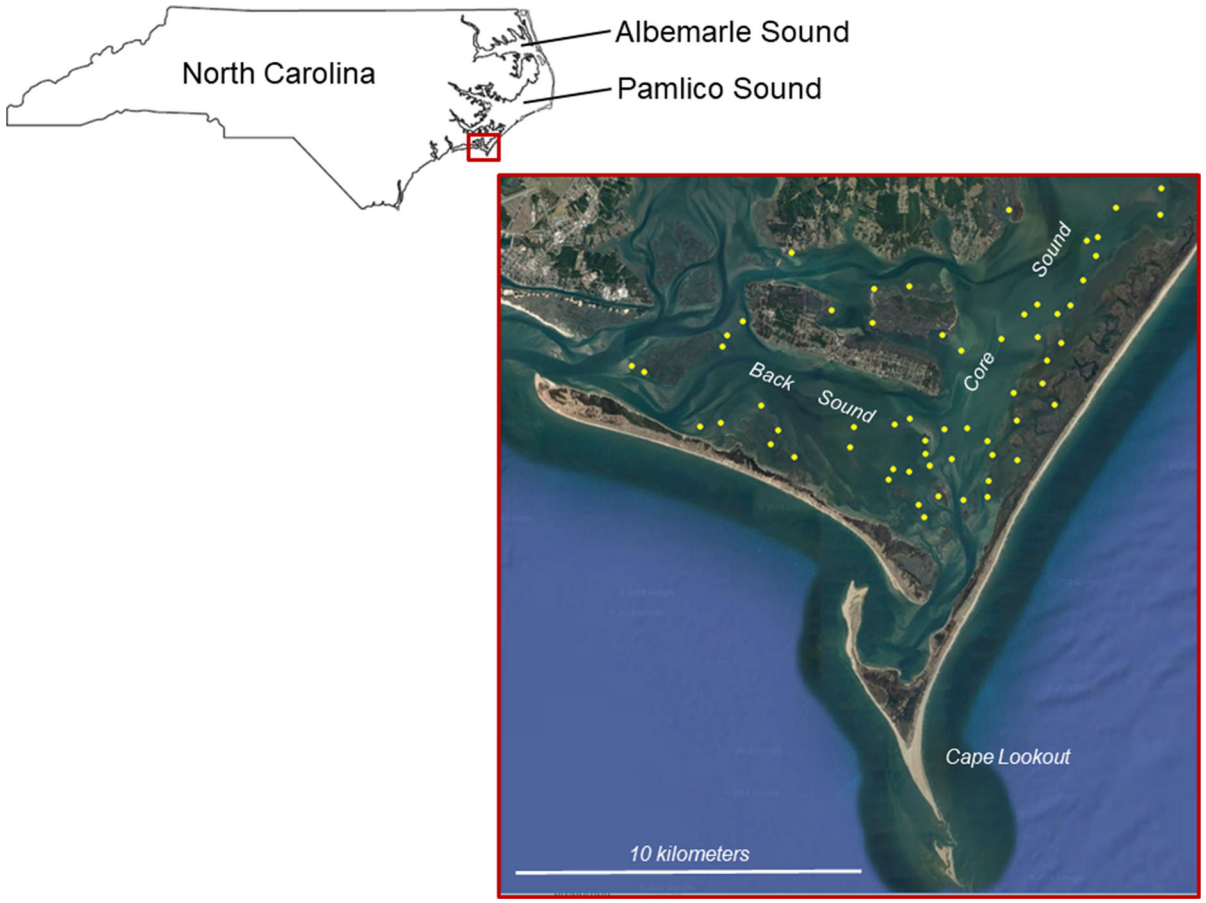

Fig. 1 Location of the 62 seagrass landscapes (yellow points) distributed throughout the southern portion of the Albemarle-Pamlico Sound Estuary System, North Carolina (Back and Core Sounds). Image from Google Earth (Landsat/Copernicus Data SIO, NOAA, U.S. Navy, NGA, GEBCO, 34.581644 N 76.380885 W)

locations where current velocity and wave action are relatively high. In areas of the estuary with greater hydrodynamic forcing, both species invest in subsurface anchoring versus canopy cover as evidenced by much lower aboveground to belowground biomass ratios (Townsend and Fonseca 1998; AVU pers. obs.). However, increased rhizome depth in response to hydrodynamic forcing has not been observed (range 1–5 cm; Townsend and Fonseca 1998; AVU pers. obs.). Bioturbation may also contribute to observed seagrass landscape patterns in this system as patchy seagrass landscapes are vulnerable to seasonal feeding activities by cownose rays (*Rhinoptera bonasus*) that target the edges of intermediate-sized patches, exposing roots and rhizomes and leaving patches more susceptible to erosion (Townsend and Fonseca 1998; Peterson et al. 2001; Fig. 2).

For both species, survival and maintenance of parent patches occurs through asexual propagation via rhizome elongation from existing patch margins, or sexually from short-distance dispersal of seeds (Fig. 2). *Z. marina* in this system exhibits both perennial and annual life history strategies as well as a combination of the two and can form transient seed banks (Jarvis et al. 2012, 2014); however, seed banks for *H. wrightii* have not been documented in this system. *Z. marina* seed densities in the Albemarle-Pamlico Sound Estuary System are lower in patchy seagrass landscapes as well as in small patches versus large patches (Livernois et al. 2017). Although vegetative shoots from both species may detach and disperse, it remains to be seen whether these fragments can successfully establish to form new patches and promote population growth (Ewanchuk and Williams

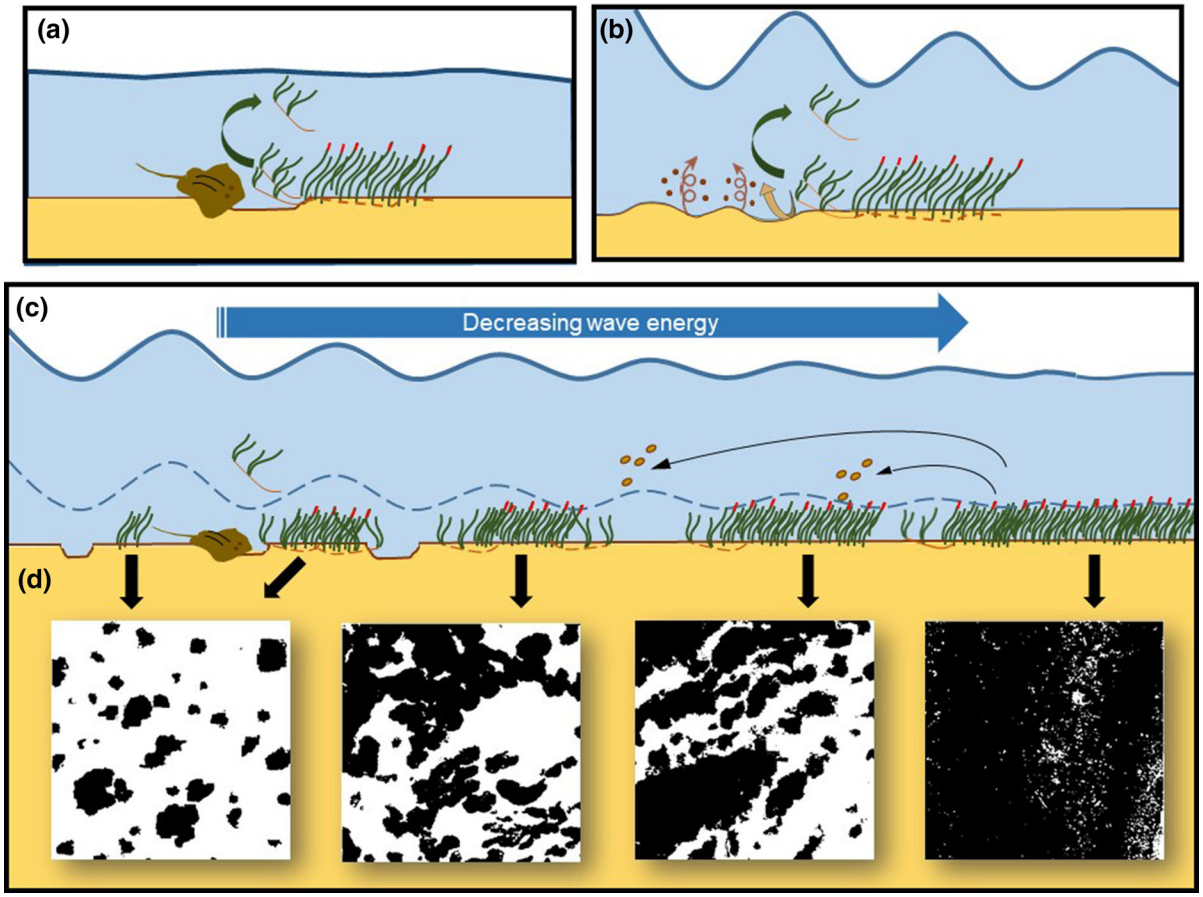

Fig. 2 Conceptual diagram of the influence of wave energy and bioturbation on seagrass landscape pattern in the Albemarle-Pamlico Sound Estuary System, North Carolina. **a** Bioturbation by sting rays exposes seagrass roots and rhizomes resulting in the uprooting, breaking, and dislodgement (green curved arrow) of seagrass shoots located along patch edges, impeding vegetative expansion. **b** In high wave energy environments, erosion (tan arrow) occurs at the margins of patches causing mobilization of sediment (brown corkscrew arrow) also resulting in the uprooting, breaking, and dislodgement (green curved arrow) of seagrass shoots located along patch edges, impeding vegetative expansion. **c** Diagrammatic representation of the wave energy gradient and associated seagrass landscape pattern. Solid blue line depicts high wave exposure (from left to right) at average water depth sites. The dashed blue line depicts a similar wave energy gradient but at shallower sites, where emersion of seagrass plants at low tide may additionally impede seagrass growth through tissue desiccation (red blade tips). Seagrass rhizome runners extend from bed margins showing vegetative propagation and patch expansion. Seed set (tan ovals), is a sporadic source of new seafloor colonization. A sting ray and ray pits at bed margins are shown in the patchier environments where ray disturbance (**a**, above) inhibits patch expansion. **d** Representative seagrass landscape (100 × 100 m) patterns observed in this study arising from the combined effects of hydrodynamic forcing and bioturbation

1996; Hall et al. 2006). However, reproductive shoots of *Z. marina* can detach and drift tens of kilometers (Harwell and Orth 2002; Reusch 2002), delivering viable seeds for subsequent patch colonization. *Z. marina* seeds ingested by fish, turtles, and seabirds can also be transported 100s to 1000s of meters prior to excretion (Sumoski and Orth 2012), providing an additional potential mechanism of long distance dispersal for this species.

Site selection via representative wave energy

We selected 62 seagrass landscapes (100 × 100 m) located at the southern end of the Albemarle-Pamlico Sound Estuary System in two smaller sounds (Core and Back Sounds; Fig. 1). Previous work on seagrass in this estuary utilized landscape extents of 50 × 50 m (Fonseca and Bell 1998; Fonseca et al. 2002). Fonseca et al. (2002) suggested that increasing

the spatial extent of seagrass landscapes would improve prediction of seagrass percent cover as a function of hydrodynamics. The size of our seagrass landscapes represents a fourfold increase in extent and greatly exceeds the spatial extent over which scale-dependent changes in seagrass percent cover occur in this area (10–20 m; Fonseca 1996; Fonseca et al. 2002). Landscapes were chosen by displaying 2013-acquired digital aerial imagery (30 × 30 cm resolution) of the Core-Back Sound area in ESRI® ArcMap™ v. 10.2.1 (ESRI 2014), overlain with an existing polygon shapefile of manually-mapped seagrass habitat (APNEP 2012) together with a hindcast of representative wave energy (RWE) generated using the Wave Exposure Model (WEMo; Malhotra and Fonseca 2007), a GIS-based hydrodynamic model. RWE represents the total wave energy in one wavelength per unit wave crest length in units of J m^{-1}. RWE is based on linear wave theory and ray tracing techniques. Using local wind speed data, WEMo computes wave height and generates waves that are propagated in the same direction along each of 56 fetch rays that are weighted to account for shoreline irregularities. Local bathymetry data are used to determine wave dissipation along the fetch rays through shoaling, wave breaking, and bottom friction. Thus, RWE represents the combined effect of wave generation, propagation, and dissipation.

Wind data were obtained from the National Data Buoy Center, Coastal-Marine Automated Network station CLKN7 (Cape Lookout, North Carolina). The ultimate spatial structure of seagrass landscapes is largely determined by wind events considered as extreme (sensu Gaines and Denny 1993; Fonseca and Bell 1998; Fonseca et al. 2000, 2002, 2008). Therefore, we used exceedance wind speeds (top five percent of wind events by wind speed; Keddy 1982), rather than averages, observed during the 3-year period May 2010 through May 2013 to compute RWE. We used the three prior years of wind data following Fonseca and Bell (1998) to encompass the lifespan of seagrasses (*Z. marina* and *H. wrightii*) found in our landscapes as captured by the aerial imagery. A spatially registered RWE grid layer was created (20 m resolution) based on existing NOAA shoreline shapefiles and bathymetry data and the wind data with each point of the grid having a value for RWE in units of J m−1. Quartiles for RWE were calculated in SAS v9.4 (SAS Institute 2013) and color-coded within the grid layer.

The seagrass polygon layer served as a boundary for clipping out all seagrass habitat from the 2013 imagery together with the respective color-coded RWE grid points. Using the Random Selection Tool in ArcMap, 15 random points were selected from within each RWE quartile. The random point served as a starting point for digitizing a square polygon with dimensions of 329 × 329 pixels (100 × 100 m). This resulted in each polygon containing 36 RWE points, each having an associated water depth (meters), from which site averages were calculated. Care was taken to ensure that all RWE points encompassed by the polygon were contained within the same quartile. Where quartile overlap occurred within the boundaries of seagrass habitat, the starting point for digitizing the polygon was adjusted by randomly choosing a direction (N-S-E-W) and selecting the next relevant quartile-specific RWE point until all RWE points encompassed by the polygon were contained within the same quartile. Two additional RWE points were chosen from the 75% quartile to adequately capture very high values for RWE. Lastly, the extent of each 100 × 100 m square polygon served as a boundary for clipping out the associated 2013 aerial imagery further to produce the representative seagrass landscapes.

Determination of tidal current speed

For each seagrass landscape, tidal current speed (cm s^{-1}) was estimated by collecting four replicate measurements of the time required for a neutrally buoyant Cyalume® ChemLight® light stick to float a linear distance of one meter at roughly 60% water depth. Current speed measurements were recorded from within the center of the seagrass landscapes. It was not possible to conduct simultaneous current speed measurements across all 62 sites or to collect current speed data at exactly peak flow (either during a tide cycle or during the year). Therefore, a number of corrections were applied to determine the maximum possible tidal current speed experienced at a given site within the tidal cycle of observations as well as the annual maximum.

Tidal current predictions were downloaded from NOAA's Center for Operational Oceanographic Products and Services (http://tidesandcurrents.noaa.gov/noaacurrents/Regions) for two subordinate current

profiler stations in the Albemarle-Pamlico Sound Estuary System: Middle Marshes (ACT6406) and Carrot Island (ACT6401). The amount of time between flood and ebb tide for the time frame encompassing the actual time of observation was computed.

The forecast change in current speed over the time from ebb to flood (or vice versa) was computed based on an assumption of a linear increase (ebb to flood) or decrease (flood to ebb) of tidal current speed with time as indicated by visual inspection of the tidal current speed prediction plots for each subordinate current profiler station (http://tidesandcurrents.noaa.gov/noaacurrents/Regions). The observed current speed was proportionally increased by a ratio, based on time to the next peak current speed. If an ebb tide, where velocity would be decreasing, the proportional amount the current speed had decreased (again, based on what percentage of the flood to ebb time period had elapsed), was added back to the observed current speed to get the forecast site maximum. To compute the predicted annual maximum current speed at a site, the ratio between the maximum current speed for that tide frame (flood, ebb) on the day of observation, and that of the annual maxima for the subordinate station was computed; the percentage increase in current speed was then applied to the observed maximum predicted current speed at that site.

Landscape pattern analysis

Seagrass cover (raster) maps for each landscape were generated using a linear spectral unmixing technique (LSU) combined with a pixel proportion threshold approach (Uhrin and Townsend 2016). Briefly, each seagrass landscape image was subjected to a forward Minimum Noise Fraction transformation (MNF, Green et al. 1988; Boardman and Kruse 1994) to increase image dimensionality. LSU was performed on each layer-stacked site image (original three band image of R, G, B + selected MNF layers) using representative sand and seagrass endmembers identified directly from images. In LSU, the measured spectrum of a mixed pixel is decomposed into its constituent endmembers and a set of corresponding image fraction planes that indicate the proportion of each endmember present in the pixel are generated. Thus, vegetation endmember fractions are proportional to the areal abundance of projected canopy cover (Roberts et al. 1993; Williams and Hunt 2002). We used a threshold approach (Arnot et al. 2004; Frazier and Wang 2011; Uhrin and Townsend 2016) to transform the sub-pixel seagrass fraction plane data into a discrete format. Statistics generated from the seagrass fraction plane were consulted to build masks (selected areas = "on") by grouping pixels with values greater than or equal to designated thresholds resulting in seagrass cover maps that were exported as rasters for use in pattern analysis. Because LSU cannot discriminate between *Z. marina* and *H. wrightii*, the seagrass maps represent the combined percent cover of both species. LSU and thresholding were performed in ENVI® v5.0 (ENVI 2012).

We selected a subset of available landscape metrics (McGarigal et al. 2012) that are ecologically relevant in seagrass systems and may affect seagrass habitat persistence as well as benthic organism distribution. Proportion of landcover (PLAND) describes seagrass landscape composition. Configuration metrics included: (1) area and edge metrics: total linear edge (TE) and area-weighted mean patch area (AREA_AM); and (2) an aggregation index describing subdivision: total number of patches (NP). For additional details on the computation and interpretation of each metric, please refer to McGarigal et al. (2012). Landscape metrics were calculated for each of the 62 seagrass maps using Fragstats 4.2 (8-neighbor rule, McGarigal et al. 2012). Area-weighted mean patch area was highly correlated with the proportion of landscape in seagrass cover and number of patches (Table 1); however, we analyzed all four metrics because each may potentially respond to different physical drivers.

Statistical analysis

Physical drivers and seagrass landscape pattern

The spatial structure of the four landscape metrics among the 62 seagrass landscapes was preliminarily evaluated using diagnostics derived from ordinary least squares regression in the software package GeoDa v1.12 (Anselin et al. 2006) and included the spatial distribution of model residuals and Moran's I. The distribution of residuals from the ordinary least squares regression displayed weak positive autocorrelation for percent cover and area-weighted mean patch size, which was corroborated by the Moran's I

Table 1 Pearson product-moment correlation coefficients (r) for physical drivers and landscape metrics among the 62 (100 × 100 m) seagrass landscapes

	Physical drivers				Landscape metrics			
	RWE	CURR	MEANZ	RWEZ	PLAND	NP	TE	AREA_AM
Physical drivers								
RWE	1.0	–	–	–	–	–	–	–
CURR	0.13	1.0	–	–	–	–	–	–
MEANZ	**− 0.79**	− 0.11	1.0	–	–	–	–	–
RWEZ	**− 0.90**	− 0.05	**0.91**	1.0	–	–	–	–
Landscape metrics								
PLAND	**− 0.67**	− 0.15	0.48	**0.53**	1.0	–	–	–
NP	**0.65**	0.08	**− 0.57**	**− 0.59**	**− 0.79**	1.0	–	–
TE	0.28	0.19	− 0.34	− 0.27	**− 0.50**	**0.64**	1.0	–
AREA_AM	**− 0.68**	− 0.06	**0.52**	**0.56**	**0.95**	**0.90**	**0.52**	1.0

Bold coefficients indicate correlations r ≥ 0.5. *RWE* representative wave energy, *CURR* mean current speed, *MEANZ* mean water depth, *RWEZ* interaction between RWE and MEANZ, *PLAND* proportion of seagrass landscape, *NP* number of patches, *TE* total edge, and *AREA_AM* area-weighted mean patch size

(0.12 and 0.09, respectively). The distribution of residuals for total edge and number of patches displayed weak negative autocorrelation, again corroborated by the Moran's I (− 0.048 and − 0.024, respectively). As no spatial structure was detected, we performed multiple linear regression using PROC REG in SAS 9.4 (SAS Institute Inc. 2013) to determine the explanatory power of representative wave energy, tidal current speed, and mean water depth on each of the four landscape metrics. Because of the close coupling between representative wave energy and water depth (Robbins and Bell 2000; Koch 2001), we tested the interaction between representative wave energy and mean water depth for all landscape metrics prior to model selection. Where the interaction was significant ($\alpha = 0.05$), it was included as an explanatory variable.

We compared models based on Akaike's information criteria (AIC; Akaike 1973; Burnham and Anderson 2002). We evaluated and ranked all possible models using a second-order bias adjustment for small sample size (AICc; Hurvich and Tsai 1989) and developed a subset of models having $\Delta_i < 2$ for model averaging. To meet assumptions of normality and homogeneity, all landscape metrics required transformation. Proportion of seagrass landscape was logit transformed (Warton and Hui 2011), total edge and number of patches were square root transformed, and area-weighted mean patch size was log transformed.

Thresholds in physical drivers

To identify potential thresholds in physical drivers, we first inspected scatter plots for those explanatory variables identified as significant in the best model for each seagrass landscape metric. If scatterplots suggested nonlinear responses in landscape metrics, we tested for its significance by comparing AIC values from the linear models to those fitted using three nonlinear functions: exponential, sigmoid logistic, and step. Nonlinear models with lower AIC values than the linear model were suggestive of a nonlinear response. Where nonlinear responses occurred, we used nonparametric deviance reduction analysis to detect change points on untransformed data (Qian et al. 2003; King et al. 2005). Nonparametric deviance reduction entails splitting a stressor-response dataset into two groups at points along the ordered stressor gradient and calculating the reduction in the response variable deviance that results from the split. The split that results in the largest reduction in the deviance is the change point. This analysis will always find a change point; thus, the identified change point must have ecological relevance. We performed the approximate Chi square test to judge whether the resulting

change point was statistically significant. Uncertainty in the change point estimate was evaluated using 95% confidence intervals calculated through bootstrapping (N = 1000). Nonparametric deviance reduction analysis was performed in R v3.4.1 using the custom package, 'ncpa' (Qian et al. 2003; R Development Core Team 2017).

Differences in seagrass landscape pattern above and below thresholds

To determine whether seagrass landscape pattern differed among landscapes from different physical driver regimes, we split the data into two groups, above and below the respective change points, and averaged the landscape metric of interest. In this way, replication across two categories of physical driver (above and below the change point) was possible in order to derive confidence intervals for comparison as suggested by Remmel and Csillag (2003). When 95% confidence intervals were overlapping, there was no significant difference among landscapes.

Patch size distribution and alternative states

We tested whether the observed frequency distribution of seagrass patch sizes in the Albemarle-Pamlico Sound Estuary System follows a power law to evaluate whether seagrass landscapes exhibit scale-free patterns, characteristic of classic critical systems. As a rule of thumb, patch size distributions that follow power laws exhibit a linear relationship on a logarithmic scale; thus, we first visually examined the frequency distribution of seagrass patch sizes within each 100 × 100 m landscape using a log–log plot. We then determined whether the power law distribution was a plausible fit to the patch size data or whether an alternative heavy-tailed distribution (e.g., many small and few large patches), the log-normal, was a better fit using the maximum likelihood method of the 'poweRlaw' package in R 3.4.1 (Clauset et al. 2009; Gillespie 2015; R Core Development Team 2017). We estimated the scaling parameter (α) of the power-law distribution, which represents the slope of the line, or the rate of decline in the number of patches with their sizes. For power laws, the scaling parameter typically, but not always, lies in the range $2 < \alpha < 3$ (Clauset et al. 2009). We also determined the lower-bound to power law behavior (scaling region), x_{min}. For each competing distribution, we plotted the complementary cumulative density function (CDF) for the patch sizes and calculated goodness of fit using the Kolmogorov–Smirnov (K-S) statistic. To assess the plausibility of power law versus log-normal, we used bootstrapping (N = 2500) to generate power-law and log-normal distributed data sets based on the values for α and x_{min} estimated from the observed data. K-S statistics were calculated for each bootstrapped data set and resulting p-values were equivalent to the proportion of time the resulting K-S statistic was larger than that of the empirical data. A distribution is considered plausible if $p > 0.1$ and the larger the p value (closer to 1), the stronger the evidence that the distribution is a good match to the data (Clauset et al. 2009). We also directly compared the power law and log-normal distributions based on log-likelihood ratios and significance values (Clauset et al. 2009) where statistical significance at $p < 0.1$ indicates a poor fit compared to the competing distribution.

Multimodality in the frequency distribution of vegetation cover is a simple indicator of the existence of alternative states (Scheffer et al. 2012). To assess whether the potential for alternative seagrass states exists in the Albemarle-Pamlico Sound Estuary System, we constructed a kernel density plot of the frequency distribution of seagrass percent cover for all 62 seagrass landscapes using the density function in R 3.4.1 (R Core Development Team 2017). A Gaussian smoothing kernel was used together with the bandwidth selection method of Sheather and Jones (1991).

Results

Maps produced from linear spectral unmixing revealed seagrass landscape patterns that ranged from complete cover to isolated seagrass patches of 0.09 m^2 separated by several meters of unvegetated sand (Supplementary Material). Some of the 100 × 100 m seagrass landscapes were composed of larger, irregularly shaped patches, with or without connections to other similarly shaped patches (Supplementary Material). Proportion of seagrass cover ranged from 4 to 100% with higher cover (> 50%) observed for lower values of representative wave energy (range 7–2347 J m^{-1}; Supplementary Material).

Physical drivers and seagrass landscape pattern

The proportion of landscape occupied by seagrass and the area-weighted mean patch size declined with increasing representative wave energy as indicated by the most supported models and model-averaged parameter estimates (Tables 2, 3). Both representative wave energy and the interaction term (representative wave energy x mean depth) were negatively correlated with proportion of landscape cover (Table 3). Together, these two variables explained 45% of the variation (Table 3). Representative wave energy explained 46% of the variation in area-weighted mean patch size. In contrast, the number of patches increased with increasing representative wave energy as indicated by the most supported models and model-averaged parameter estimates (Tables 2, 3). Representative wave energy explained 42% of the variation in number of patches (Table 3). Total edge declined with increasing mean water depth (Tables 2, 3). Mean water depth was significantly negatively correlated with total edge but explained only 10% of the variation (Table 3).

Thresholds in physical drivers

Scatterplots revealed potential nonlinear relationships between representative wave energy and three landscape metrics: proportion of landscape, number of patches, and area-weighted mean patch size (Fig. 3). For all three landscape metrics, the model fitted with a sigmoid logistic function had the lowest AIC value (sigmoid value vs linear value). Nonparametric deviance reduction analysis suggested that changes in both proportion of landscape and area-weighted mean patch size occurred at a representative wave energy value of 679 J m^{-1} (95% CI 675, 705; Fig. 3). Changes in the number of patches occurred at a representative wave energy value of 774 J m^{-1} (95% CI 675, 1153; Fig. 3).

Differences in seagrass landscape pattern above and below thresholds

Seagrass landscapes differed in their spatial configuration and in their physical environment, above and below the representative wave energy change point of 679 J m^{-1} (Fig. 4). Above the change point, seagrass landscapes experienced greater wave energy and were deeper than landscapes below the change point (Fig. 4). In addition, seagrass landscapes above the change point had less proportional cover and more patches that were smaller in size than landscapes below the change point (Fig. 4). Tidal current speed (not presented) was not different between seagrass landscapes above and below the change point.

Patch size distribution and alternative states

Patch size distributions for individual seagrass landscapes formed power-law distributions over a broad range of seagrass landscape proportion both above and

Table 2 Model selection statistics for physical driver effects on four seagrass landscape metrics

Model	AIC_c	Δ_i	ω_i
Proportion of seagrass landscape			
Wave energy, wave energy × mean depth	− 0.45	0	0.47
Wave energy	0.22	0.67	0.33
Wave energy, mean depth, wave energy × mean depth	1.24	1.69	0.20
Total edge			
Mean depth	293.75	0	0.62
Current speed, mean depth	294.70	0.95	0.38
Area-weighted mean patch size			
Wave energy	− 28.41	0	0.40
Wave energy, mean depth, wave energy × mean depth	− 27.94	0.47	0.31
Wave energy, wave energy × mean depth	− 27.77	0.64	0.29
Number of patches			
Wave energy	− 11.20	0	0.61
Wave energy, wave energy × mean depth	− 10.27	0.93	0.39

The best approximating model based on corrected Akaike Information Criterion (AIC_c) is followed in rank order by those models having substantial support ($\Delta_i < 2$). (Δ_i= AIC differences, ω_i= Akaike weights)

Table 3 Model-averaged parameter estimates (β), unconditional standard errors (SE), 95% lower (CI_L) and upper (CI_U) confidence intervals, p values, and adjusted R^2 (adj R^2) for the AIC_c-selected best model for physical driver effects on four seagrass landscape metrics

	β	SE	CI_L	CI_U	p	adj R^2
Proportion of landscape						
Intercept	1.36	0.13	1.10	1.62	< 0.0001	0.45
Wave energy	− 0.002	0.0003	− 0.002	− 0.001	< 0.0001	
Wave energy × mean depth	− 0.0005	0.0001	− 0.0007	− 0.0003	0.09	
Total edge						
Intercept	31.84	15.42	1.77	61.91	< 0.0001	0.10
Mean depth	− 9.49	5.81	− 20.83	1.84	0.01	
Number of patches						
Intercept	4.38	2.07	0.35	8.41	< 0.0001	0.41
Wave energy	0.004	0.002	0.0003	0.008	< 0.0001	
Area-weighted mean patch size						
Intercept	− 2.83	1.35	0.19	5.47	< 0.0001	0.46
Wave energy	− 0.001	0.0007	− 0.003	0.00002	< 0.0001	

below the identified wave exposure change point (Fig. 5). Of the 50 seagrass landscapes having sufficient sample size (i.e., enough patch size frequencies) to perform a power law analysis, 88% exhibited plausibility of power-distributions ($p > 0.1$) with estimated scaling exponents falling within the range typically observed in power law, $2 < \alpha < 3$ (Fig. 5).

The frequency distribution of seagrass percent cover appears bimodal, with peaks at both high and low percent cover, corresponding to high and low values for representative wave energy, and suggesting the possible existence of alternative stable states in this system (Fig. 6). Over intermediate values of representative wave energy, including in the range of the estimated threshold, the two states can coexist.

Discussion

We used fine-resolution data on seagrass cover of two co-dominant species to identify thresholds in physical drivers associated with qualitative changes in seagrass spatial pattern. We identified a change point in representative wave energy, a hydrodynamic driver based on exceedance wind events, in the Albemarle-Pamlico Sound Estuary System. The change point was associated with changes in the composition and configuration of seagrass landscapes, namely percent cover, patch size, and number of patches. At the change point and beyond, wave energy reaches a level where presumably sediment erosion exceeds the ability of seagrass to stabilize the seafloor with a consequence of uprooting plants and loss of landscape cover. Our identified wave energy change point corroborates the observations of Fonseca and Bell (1998), who, over two decades ago, suggested thresholds in representative wave energy (range 450–750 J m^{-1}) and tidal current speed (25 cm s^{-1}) in this system. These authors reported discernible differences in seagrass percent cover, perimeter to area ratio, and sediment composition when these thresholds were exceeded. However, the authors deliberately selected sites (50 × 50 m) based on visually perceived gradients of seagrass patchiness observed from aerial photographs and mapped the spatial pattern of these landscapes in situ at 1 m^2 resolution (Fonseca and Bell 1998). Our study of seagrass landscapes in this system substantially increased the number and extent of landscapes and analysis of landscape pattern was performed at over 3 × the resolution, 4 × the extent per site and at 3.4 × as many sites as the previous work. Importantly, we chose our landscapes via a stratified site selection process founded on quartiles of representative wave energy, ensuring that the relationship between wave energy and seagrass landscape was not inherently biased. Here, previous

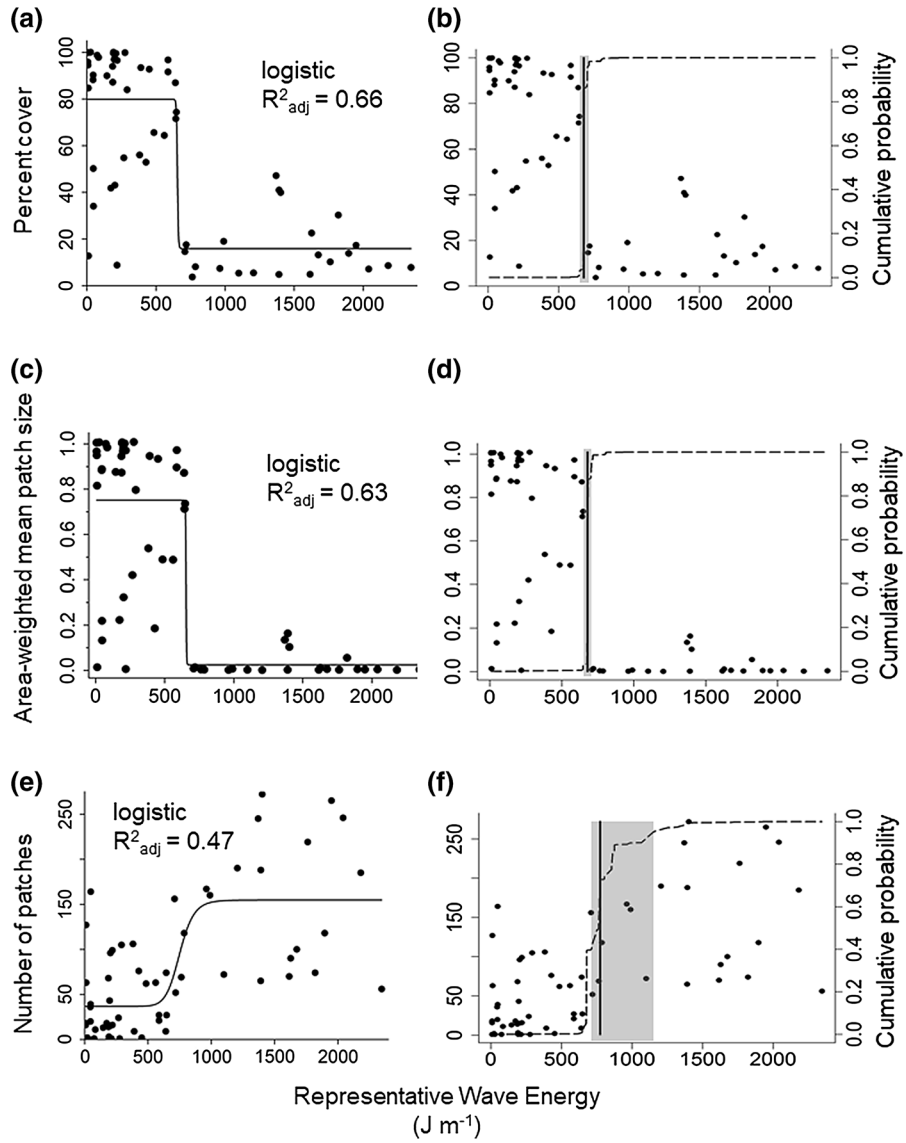

Fig. 3 Nonlinear responses of proportion of seagrass landscape (percent cover), area-weighted mean patch size, and number of patches to representative wave energy. The left panels (**a**, **c**, **e**) are scatterplots of each landscape metric fitted by a sigmoid logistic function. The right panels (**b**, **d**, **f**) are the resulting change points estimated by nonparametric deviance reduction with shaded 95% confidence intervals estimated via bootstrapping (N = 1000)

observations of apparent threshold behavior driven by wind-wave exposure have now been clearly identified and statistically verified apart from the influence of tidal currents.

Seagrass percent cover increased nearly monotonically with decreasing wave energy. Seagrass landscapes having very low wave energy and often located in shallow waters adjacent to the mainland or fringing large marsh islands, formed continuous meadows with high percent cover ($\sim$ 75%). However, there was a slight trend of decreasing seagrass cover as water depth became shallower, concomitant with a minor positive interaction between the shallowest depths and the highest representative wave energy that decreased cover further. Thus, shallow shoals exposed to high wave energy had the least seagrass cover, expressed as small, well-dispersed patches. On these shoals, seagrass may be additionally influenced by high summer temperatures and emersion, especially during extreme low tides, as observed for other temperate seagrass ecosystems (Moore and Jarvis 2008; van der Heide et al. 2010; Carr et al. 2012a; Moore et al. 2014).

In the Albemarle-Pamlico Sound Estuary System, *Zostera marina* and *Halodule wrightii* intermingle at the sub-meter scale and sometimes down to the 1 cm scale. Therefore, it is not possible to discriminate

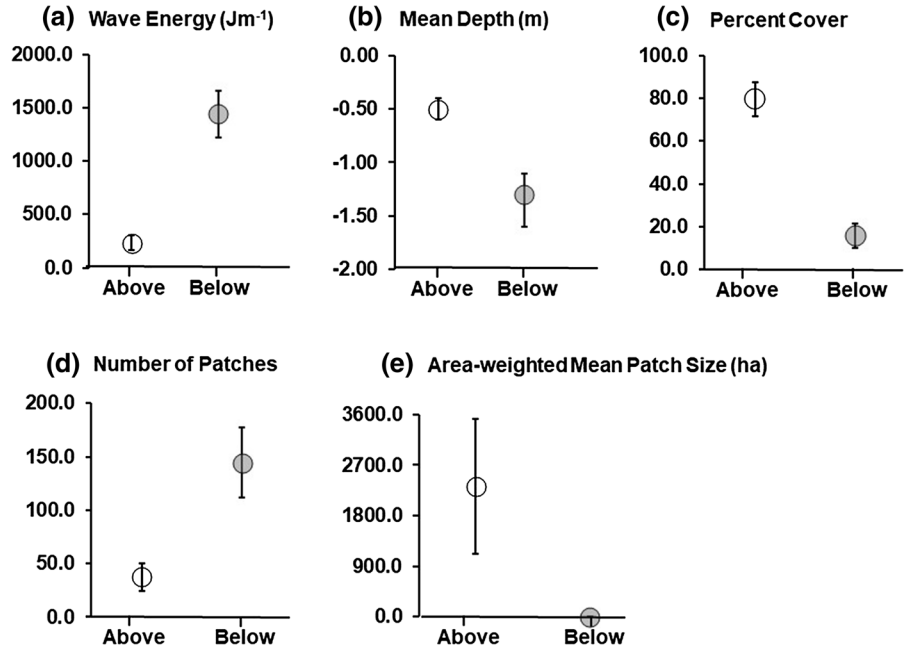

Fig. 4 The 95% statistical confidence intervals above (gray) and below (white) the identified change points for representative wave energy (**a**), mean depth (**b**), proportion of seagrass landscape (**c**), area-weighted mean patch size (**d**), and total number of patches (**e**). Circles indicate the mean value

species-specific effects on landscape pattern as related to wave energy. Although multi-species seagrass landscapes are not rare globally, it is rare that these two particular species overlap. Although this study focuses on a specific seagrass ecosystem, the approach used here can be exported to other seagrass ecosystems where the relationship between landscape pattern and hydrodynamics is suggested and mapping data are available.

The seasonal interplay of the two codominant seagrass species of the Albemarle-Pamlico Sound Estuary System might confer resilience or increase vulnerability upon this seagrass ecosystem in the face of extreme wind events. In locations where *Z. marina* and *H. wrightii* coexist, their seasonal displacement of peak growth periods results in a seagrass canopy and rhizome mat that is present in an active state for much of the year, enhancing sediment stabilization in those areas. An additional boost to sediment stabilization is the increased investment to belowground biomass versus canopy cover observed for both species in areas where hydrodynamic forcing is high (Townsend and Fonseca 1998; AVU pers. obs.). Although peak biomass is not simultaneous, there is some converging abundance in early summer and early fall. During those times of the year, it is possible that resilience to storms is greater due to the combined biomass and the comparable abilities of the two species for reducing flow speed through their respective canopies (i.e., similar resistance to sediment movement; Fonseca and Fisher 1986). Gurbiscz et al. (2016) demonstrated that the effects of tropical cyclones were mitigated when storms occurred during the simultaneous peak biomass (summer) of four codominant species located in the tidal freshwater upper Chesapeake Bay. Having attained maximum plant height and density increased the capability of the bed for attenuating wind-driven wave energy, which reduced sediment resuspension (less turbidity, greater light penetration) and diverted flow around the bed which prevented erosion from reaching into the core of the bed (Gurbiscz et al. 2016). This mechanism not only reduced within-patch vulnerability, but was theorized to have conferred among-patch resiliency through the "spillover" of clearer water to adjacent impacted areas where plant loss was more substantial (Gurbiscz et al. 2016).

In areas of the estuary where *Z. marina* and *H. wrightii* exist monotypically, the capacity for resilience may be reduced and vulnerability enhanced. It is possible that shallow depths select against *Z. marina*, leaving *H. wrightii* to be a seasonal dominant (especially during hurricane season) and it is unknown whether the absence of *Z. marina* could leave *H. wrightii* more vulnerable to disturbance. However, the absence of *Z. marina* means that *H. wrightii* may perhaps more fully exploit local resources (Micheli

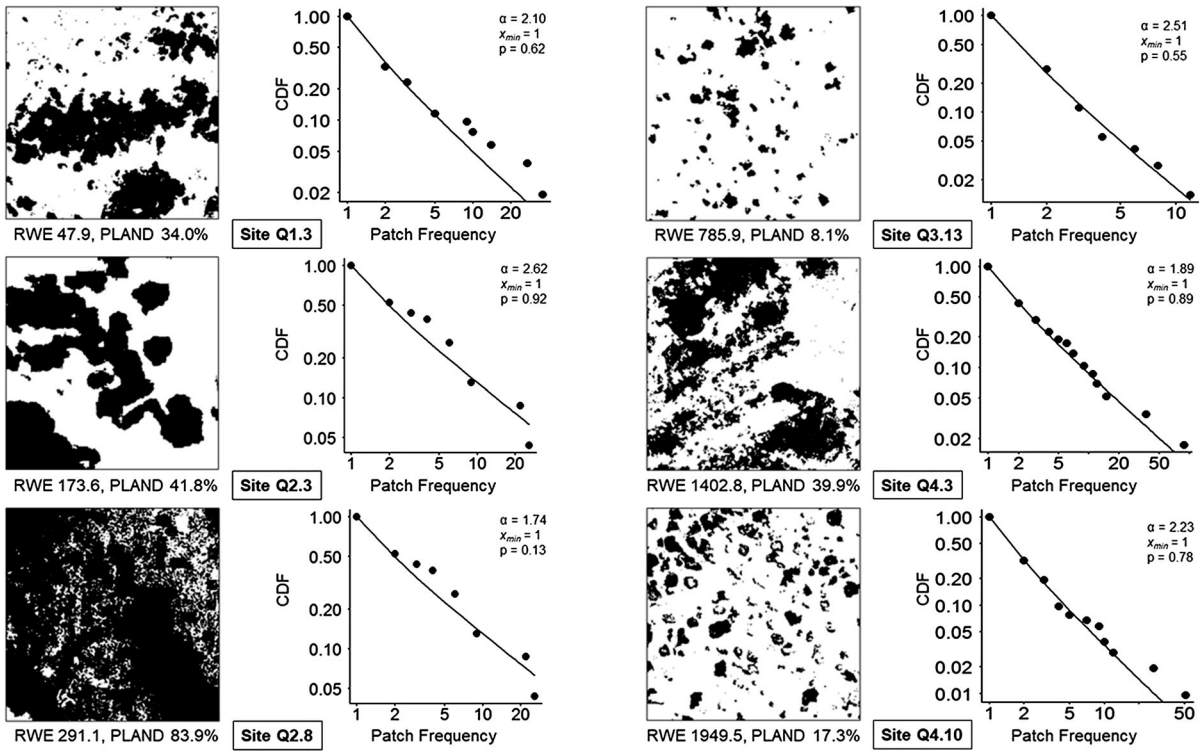

Fig. 5 Landscape percent cover and associated power law analysis for a selection of seagrass landscapes in the Albemarle-Pamlico Estuary System exhibiting power law bevavior. The left side of each panel contains binary maps of seagrass percent cover, in which black pixels indicate seagrass presence. Landscape extent is 100 × 100 m with a resolution of 0.3 m. The right side of each panel corresponds to the cumulative distribution functions (CDFs; y-axis) and their maximum likelihood power law fit for the frequency distribution of patch sizes for a selection of seagrass landscapes examined in the study

et al. 2008). We have observed monospecific *H. wrightii* beds on the shallow, wave-influenced shoals to have a prodigious belowground biomass not apparent in low energy regimes (similarly for *Z. marina* when it is monotypic, although shallow monotypic *Z. marina* is not a persistent feature at this limit of its distribution). In addition, Livernois et al. (2017) reported a negative effect of *H. wright* shoot density on the density of *Z. marina* seeds. The lost 'benefit' of a dual-species bed versus the 'gain' achieved via resource exploitation in a monotypic bed may offset one another. This type of dual-species influence warrants further investigation but may be limited in that the presence of seagrass beds across gradients of water depth and energy are not orthogonal; not all combinations of seagrass species, water depth and wave energy exist in this estuary. To confound the issue further, where the two species exist in isolation, they experience a different suite of environmental conditions that cannot inform what they might do when they are interspersed. Thus, their resilience and vulnerability may even out across these gradients of conditions but this requires further investigation.

Although not examined here, differential responses to burial between *Z. marina* and *H. wrightii* may also contribute to spatial patterning in seagrass landscapes. Results from a handful of burial experiments indicate that resilience to burial is species-specific, largely a function of seagrass plant size and the ability of unburied shoots to translocate resources to buried shoots (Duarte et al. 1997; Cabaço et al. 2008; Ooi et al. 2011). Mills and Fonseca (2003) conducted field experiments where *Z. marina* in our study location experienced 50% mortality when buried to 25% of aboveground height. Surviving plants exhibited decreased productivity and leaf length suggesting that even low levels of burial, may inhibit compensatory

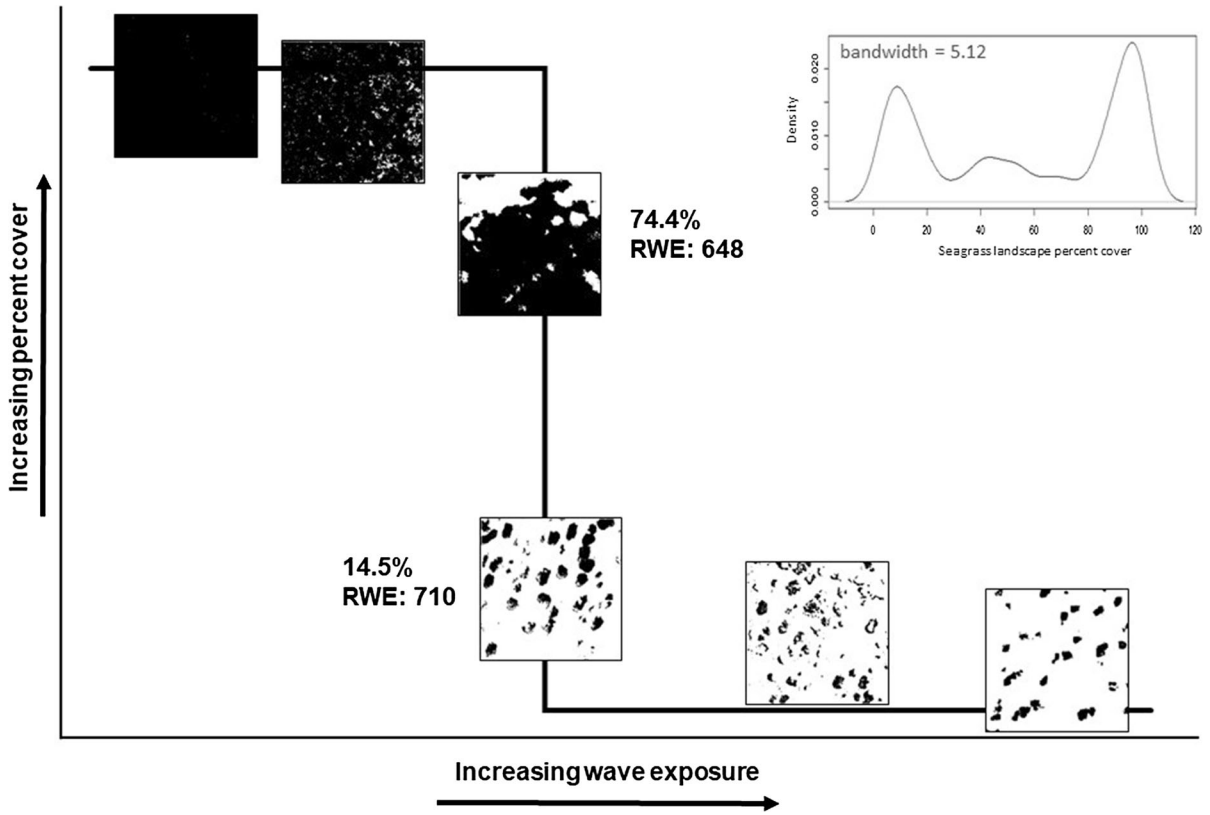

Fig. 6 Conceptual diagram showing potential bistability in seagrass landscapes of the Albemarle-Pamlico Sound Estuary System where landscapes near identified thresholds in representative wave energy can have both high and low percent cover. Inset: Kernel density estimation of the frequency distribution of seagrass percent cover in 100 × 100 m grid cells. There are two distinct nodes corresponding to contiguous seagrass landscapes and those exhibiting high numbers of small patches

recovery via leaf elongation (Mills and Fonseca 2003). We are unaware of any burial studies specific to *H. wrightii*. However, Ooi et al. (2011) reported on burial in the congener, *Halodule uninervis* (tropical southeast Asia) having similar morphology and physiology. The overall effect of burial was a loss of shoots and a reduction in the size of shoots and rhizomes with significant effects apparent at burial depths greater than 20% plant height (Oi et al. 2011). *H. uninervis* was also unable to translocate sufficient resources from unaffected shoots to buried shoots, suggesting a reduced capacity for responding to burial events compared to the other species examined (Ooi et al. 2011). Thus, plant responses to burial at various temporal and spatial scales, as may occur during storm events, may influence spatial heterogeneity in seagrass landscapes, although the exact mechanisms remain unidentified.

Patch size distributions from seagrass landscapes across a wave energy gradient were examined as a potential indicator of vulnerability to a landscape state change. Our analysis of patch size distribution for seagrass landscapes in the Albemarle-Pamlico Sound Estuary System indicates moderate support for a power law relationship across a wide range of individual seagrass landscape covers and wave energy regimes. Power laws have been used to reveal critical thresholds in vegetation patterns that may signify potential landscape degradation in various ecosystems including arid scrubland/grassland (Kéfi et al. 2007; Scanlon et al. 2007), neotropical and deciduous forests (Kizaki and Katori 1999), intertidal mussel beds (Guichard et al. 2003), intertidal mudflat diatom films (Weerman et al. 2012), and Everglades sawgrass (Casey et al. 2016). To our knowledge, power laws have not been applied to patch-size distributions in

seagrass landscapes and this warrants further investigation into how critical dynamics in this system might generate the observed power law distribution and whether power law adherence may presage a state shift in coverage and abundance.

Patchiness in seagrass landscapes may also arise from self-organizing processes, similar to patterns observed in terrestrial vegetation, particularly for arid systems (Rietkerk et al. 2002). Ruiz-Reynés et al. (2017) developed a simple model based on clonal plant growth that reproduced naturally occurring seagrass patterns for *Posidonia oceanica* ranging from isolated fairy circles (gaps), and bands to "leopard skin" (small seagrass patches on a bare sand landscape). These patterns were a result of variable shoot mortality along with facilitative and competitive interactions among seagrass shoots (Ruiz-Reynés et al. 2017). Regular banded patterns of *Zostera noltii* observed in Saint Efflam Bay, France were attributed to local positive and long-range negative feedbacks between hydrodynamics and seagrass shoot growth (van der Heide et al. 2010). High root density improves anchoring and sediment stabilization and prevents dislodgement while the canopy causes scouring that intensifies with distance through a banded patch. Although self-organizing processes were not examined in our study, given the observation of enhanced belowground biomass in seagrass patches exposed to high hydrodynamic forcing, it is possible that self-organization may contribute to spatial patterning in this system.

Our observation of bimodality in the frequency distribution of seagrass cover in the Albemarle-Pamlico Sound Estuary System adds to mounting evidence for the existence of alternative states (bistability) in seagrass landscapes (van der Heide et al. 2007, 2010, 2011, 2012; Carr et al. 2010, 2012a, b, 2016; Christianen et al. 2014; Maxwell et al. 2015; Adams et al. 2016). Alternative states of continuous seagrass cover versus a spatial mosaic (seagrass banded pattern) have been attributed to feedbacks between seagrass presence, suspended sediment, and benthic light availability (linked to water depth and hydrodynamic regime; van der Heide et al. 2010). Feedbacks have been modeled between seagrass growth, biological activity (e.g., grazing), and rates of sediment accretion/erosion that have generated alternative states of bare landscapes versus a spatial mosaic (water-saturated depressions alternating with emmersed seagrass-vegetated hummocks: van der Heide et al. 2012; unvegetated gaps: Christianen et al. 2014). Although not directly examined in this study, it is possible that similar feedbacks are operating in our study system. Cownose rays foraging in seagrass landscapes target the edges of intermediate-sized patches, exposing roots and rhizomes and leaving patches more susceptible to erosion (Townsend and Fonseca 1998; Peterson et al. 2001). Thus, ray foraging may reduce the size of patches in an already patchy landscape or eliminate patches altogether creating additional bare substrate.

Identification of threshold behavior and alternative states can inform seagrass ecosystem management particularly under climate scenarios where the frequency, duration, and intensity of extreme weather events known to inflict seagrass loss are predicted to increase (tropical cyclones: Knutson et al. 2010; Christensen et al. 2013; Villarini and Vecchi 2013; extreme warm temperatures: Coumou and Rahmstorf 2012; Perkins et al. 2012; Hobday et al. 2016). Many coastal seagrass ecosystems, including the Albemarle Pamlico Sound Estuary System, are susceptible to tropical cyclones and winter storms, which can cause rapid, catastrophic loss of seagrass cover and affect resilience (Fonseca et al. 2000; Gera 2013; Gurbiscz et al. 2016). Warm temperature extremes have also been implicated in severe biomass loss in other temperate seagrass ecosystems (Chesapeake Bay: Moore and Jarvis 2008; Moore et al. 2014; Australia: Thomson et al. 2015). Thus, the existence of many small and few large seagrass patches could leave a system vulnerable to future extreme climatic events that could eliminate existing patchy seagrass landscapes within the estuary and shift remaining patch size distribution to more and smaller patches, resulting in more frequent changes among alternative states from vegetated to unvegetated. Similar to the predictive model of habitat suitability based on susceptibility to storms by Kelly et al. (2001), this study revealed that a substantial portion of the estuarine seafloor in this region is composed of patchy seagrass beds and that a threshold patchiness exists at a given wave energy exposure. With climate change and its associated increases in weather extremes, much of this estuarine seagrass coverage will be exposed to increased wave energy disturbance. In fact, Kelly et al. (2001) predicted that 16% of the seagrass in this study area is highly susceptible to acute storm events.

For those portions of the seafloor that have seagrasses and are just below the wave energy threshold, such increases in wave energy could tip those habitats into a new stable state of lower cover resulting in less seagrass cover overall in the estuary. Such a net decline in seagrass cover may in turn lead to reductions in several ecosystem services associated with seagrass (Nordlund et al. 2016) particularly as faunal utilization appears to scale to seagrass acreage and less so to patch size (Boström et al. 2006, 2011; Lefcheck et al. 2016). Thus, understanding the distribution of seagrass cover and its patchiness as indicators of system change in the face of external drivers such as climate change may in turn inform a cascade of changes in ecosystem service availability.

Acknowledgements Funding was provided to AVU by the NOAA National Ocean Service Coastal Science Board with indirect support from the NOAA National Centers for Coastal Ocean Science, the NOAA Office of Response and Restoration, and the University of Wisconsin-Madison. MGT acknowledges support from the University of Wisconsin Vilas Trust and UW2020 initiative. We are immensely grateful to M. Fonseca for invaluable insights regarding hydrodynamic properties of seagrass beds and historical knowledge of the seagrass ecosystem in the Albemarle-Pamlico Sound Estuary System, and for critical review of earlier versions of the manuscript. We appreciate statistical consultation and R code provided by J. Qiu. Aerial imagery was generously provided by the Albemarle-Pamlico National Estuary Partnership. We thank W. Rogers for organizing the current speed measurements in the field. We benefited from discussion with S. Carpenter, E. Damschen, P. Townsend and J. Zedler. We appreciated and incorporated suggestions from the anonymous reviewers assigned by the journal. The views expressed here do not necessarily reflect those of NOAA.

References

Adams MP, Saunders MI, Maxwell P, Tuazon D, Roelfsema CM, Callaghan DP, Leon J, Grinham AR, O'Brien KR (2016) Prioritizing localised management actions for seagrass conservation and restoration using a species distribution model. Aquat Conserv: Mar Freshw Ecosyst 26:639–659

Akaike H (1973) Information theory as an extension of the maximum likelihood principle. In: Petrov BN, Csaki F (eds) Second international symposium on information theory. Budapest, Hungary, pp 267–281

Anselin L, Syabri I, Kho Y (2006) GeoDa: an introduction to spatial data analysis. Geogr Anal 38:5–22

APNEP (Albemarle-Pamlico National Estuary Partnership) (2012) 2012 Albemarle-Pamlico Ecosystem Assessment. Albemarle-Pamlico National Estuary Partnership, North Carolina Department of Environmental Quality, Raleigh, North Carolina. http://portal.ncdenr.org/web/apnep/reports

Arnot C, Fisher PF, Wadsworth R, Wellens J (2004) Landscape metrics with ecotones: pattern under uncertainty. Landscape Ecol 19:181–195

Biber P, Gallegos CL, Kenworthy WJ (2008) Calibration of a bio-optical model in the North River, North Carolina (Albemarle-Pamlico Sound): a tool to evaluate water quality impacts on seagrasses. Estuar Coasts 31:177–191

Boardman JW, Kruse FA (1994) Automated spectral analysis: a geologic example using AVIRIS data, North Grapevine Mountain, Nevada. Proceedings ERIM Tenth Thematic Conference on Geologic Remote Sensing. Michigan, Ann Arbor, pp 407–418

Boström C, Jackson EL, Simenstad CA (2006) Seagrass landscapes and their effects on associated fauna: a review. Estuar Coast Shelf Sci 68:383–403

Boström C, Pittman SJ, Simenstad C, Kneib RT (2011) Seascape ecology of coastal biogenic habitats: advances, gaps, and challenges. Mar Ecol Prog Ser 427:191–217

Burnham KP, Anderson DR (2002) Model selection and multimodel inference. Springer, New York

Cabaço S, Santos R, Duarte CM (2008) The impact of sediment burial and erosion on seagrasses: a review. Estuar Coast Shelf Sci 79:354–366

Carr J, D'Odorico P, McGlathery K, Wiberg L (2010) Stability and bistability of seagrass ecosystems in shallow coastal lagoons: role of feedbacks with sediment resuspension and light attenuation. J Geophys Res 115:G03011

Carr JA, D'Odorico P, McGlathery KJ, Wiberg PL (2012a) Modeling the effects of climate change on eelgrass stability and resilience: future scenarios and leading indicators of collapse. Mar Ecol Prog Ser 448:289–301

Carr JA, D'Odorico P, McGlathery KJ, Wiberg PL (2012b) Stability and resilience of seagrass meadows to seasonal and interannual dynamics and environmental stress. J Geophys Res 117:G01007

Carr JA, D'Odorico P, McGlathery KJ, Wiberg PL (2016) Spatially explicit feedbacks between seagrass meadow structure, sediment and light: habitat suitability for seagrass growth. Adv Water Resour 93:315–325

Casey ST, Cohen MJ, Acharya S, Kaplan DA, Jawitz JW (2016) Hydrologic controls on aperiodic spatial organization of the ridge-slough patterned landscape. Hydrol Earth Syst Sci 20:4467–4467

Christensen JH, Kumar KK, Aldrian E, An SI, Cavalcanti IFA, de Castro M, Dong W, Goswami P, Hall A, Kanyanga JK, Kitoh A, Kossin J, Lau N-C, Renwick J, Stephenson DB, Xie S P, Zhou T (2013) Climate phenomena and their relevance for future regional climate change. In: Stocker TF, Qin D, Plattner G-K, Tignor M, Allen SK, J Boschung J, Nauels A, Xia Y, Bex V, Midgley PM (eds.), Climate Change 2013: the physical sci-ence basis. Contribution of working group I to the fifth assessment report of the Intergovernmental Panel on Climate Change, Cambridge University Press, Cambridge, United Kingdom and New York, pp 14SM1-14SM62

Christianen MJA, Herman PMJ, Bouma TJ, Lamers LPM, van Katwijk MM, van der Heide T, Mumby PJ, Silliman BR, Engelhard SL, van de Kerk M, Kiswara W, van de Koppel J (2014) Habitat collapse due to overgrazing threatens turtle

conservation in marine protected areas. Proc R Soc B 281:20132890
Clauset A, Shalizi CR, Newman MEJ (2009) Power-law distributions in empirical data. SIAM Rev 51(4):661–703
Coumou D, Rahmstorf S (2012) A decade of weather extremes. Nat Clim Change 2:491–496
den Hartog C (1971) The dynamic aspect in the ecology of seagrass communities. Thalass Jugosl 7:101–112
Dennison W, Orth R, Moore K, Stevenson V, Kollar S, Bergstrom P, Batuik RA (1993) Assessing water quality with submersed aquatic vegetation. Bioscience 43:86–95
Dewsbury BM, Bhat M, Fourqurean JW (2016) A review of seagrass economic valuations: gaps and progress in valuation approaches. Ecosyst Serv 18:68–77
Duarte CM, Terrados J, Agawin NSR, Fortes MD, Bach S, Kenworthy WJ (1997) Response of a mixed Philippine seagrass meadow to experimental burial. Mar Ecol Prog Ser 147:285–294
ENVI (2012) ENVI 5.0 software package. Harris Geospatial Solutions, Bloomfield, Colorado
ESRI (2014) ArcMap 10.2.1 software package. Environmental Systems Research Institute, Redmonds, California
Ewanchuk PJ, Williams SL (1996) Survival and re-establishment of vegetative fragments of eelgrass (*Zostera marina*). Can J Bot 74:1584–1590
Ferguson RL, Korfmacher K (1997) Remote sensing and GIS analysis of seagrass meadows in North Carolina, USA. Aquat Bot 58:241–258
Ferguson RL, Wood LL, Graham DB (1993) Monitoring spatial change in seagrass habitat with aerial photography. Photogramm Eng Remote Sens 59:1033–1038
Fonseca MS (1996) Scale dependence in the study of seagrass systems. In: Pages 95-104 in Kuo J, Phillips RC, Walker D I, Kirkman H (eds) Seagrass biology: proceedings of an international workshop, January 25-29, Rottnest Island, Western Australia. Faculty of Sciences, University of Western Australia, Crawley, Western Australia, pp 95-104
Fonseca MS, Bell SS (1998) Influence of physical setting on seagrass landscapes near Beaufort, North Carolina, USA. Mar Ecol Prog Ser 171:109–121
Fonseca MS, Fisher JS (1986) A comparison of canopy friction and sediment movement between four species of seagrass with reference to their ecology and restoration. Mar Ecol Prog Ser 29:15–22
Fonseca MS, Kenworthy WJ, Griffith E, Hall MO, Finkbeiner M, Bell SS (2008) Factors influencing landscape pattern of the seagrass *Halophila decipiens* in an oceanic setting. Estuar Coast Shelf Sci 76:163–174
Fonseca MS, Kenworthy WJ, Whitfield PE (2000) Temporal dynamics of seagrass landscapes: a preliminary comparison of chronic and extreme disturbance events. Biol Mar Medit 7(2):373–376
Fonseca MS, Whitfield PE, Kelly NM, Bell SS (2002) Modeling seagrass landscape pattern and associated ecological attributes. Ecol Appl 12:218–237
Fonseca MS, Zieman JC, Thayer GW, Fisher JS (1983) The role of current velocity in structuring eelgrass (*Zostera marina* L.) meadows. Estuar Coast Shelf Sci 17:367–380
Frazier AE, Wang L (2011) Evaluation of soft classifications for characterizing spatial patterns of invasive species. Remote Sens Environ 115:1997–2007
Gaines SD, Denny MW (1993) The largest, smallest, highest, lowest, longest, and shortest: extremes in ecology. Ecology 74:1677–1692
Gera A (2013) Landscape fragmentation and resilience in seagrass meadows. Dissertation, University of Barcelona
Gillespie CS (2015) Fitting heavy tailed distributions: the poweRlaw package. J Stat Softw 64(2):i02
Green AA, Berman M, Switzer B, Craig MD (1988) A transformation for ordering multispectral data in terms of image quality with implications for noise removal. IEEE Trans Geosci Remote Sens 26:65–74
Groffman PM, Baron JS, Blett T, Gold AJ, Goodman I, Gunderson LH, Levinson BM, Palmer MA, Paerl HW, Peterson GD, Poff NL, Rejeski DW, Reynolds JF, Turner MG, Weathers KG, Wiens J (2006) Ecological thresholds: the key to successful environmental management or an important concept with no practical application? Ecosystems 9:1–13
Guénette JS, Villard MA (2004) Do empirical thresholds truly reflect species tolerance to habitat alteration? Ecol Bull 51:163–171
Guénette JS, Villard MA (2005) Thresholds in forest bird response to habitat alteration as quantitative targets for conservation. Conserv Biol 19:1168–1180
Guichard F, Halpin PM, Allison GW, Lubchenco J, Menge BA (2003) Mussesl disturbance dynamics: signatures of oceanographic forcing from local interactions. Am Nat 161:889–904
Gurbiscz C, Kemp MW, Sanford LP, Orth RJ (2016) Mechanisms of storm-related loss and resilience in a large submersed plant bed. Estuar Coasts 39:951–966
Hall L, Hanisak MD, Virnstein RW (2006) Fragments of the seagrasses *Halodule wrightii* and *Halophila johnsonii* as potential recruits in Indian River Lagoon, Florida. Mar Ecol Prog Ser 310:109–117
Harwell MC, Orth RJ (2002) Long distance dispersal potential in a marine macrophyte. Ecology 83:3319–3330
Hobday AJ, Alexander LV, Perkins SE, Smale DA, Straub SC, Oliver ECJ, Benthuysen JA, Burrows MT, Donat MG, Feng M, Holbrook NJ, Moore PJ, Scannell HA, Gupta AS, Wernberg T (2016) A hierarchical approach to defining marine heatwaves. Prog Oceanogr 141:227–238
Hurvich CM, Tsai CL (1989) Regression and time series model selection in small samples. Biometrika 76:297–307
Jarvis JC, Moore KA, Kenworthy WJ (2012) Characterization and ecological implication of eelgrass life history strategies near the species' southern limit in the western North Atlantic. Mar Ecol Prog Ser 444:43–56
Jarvis JC, Moore KA, Kenworthy WJ (2014) Persistence of *Zostera marina* L. (eelgrass) seeds in the sediment seed bank. J Exp Mar Biol Ecol 459:126–136
Keddy PA (1982) Quantifying within-lake gradients of wave energy: interrelationships of wave energy, substrate particle size and shoreline plants in Axe Lake, Ontario. Aquat Bot 14:41–58
Kéfi S, Guttal V, Brock WA, Carpenter SR, Ellison AM, Livina VN, Seekell DA, Scheffer M, van Nes EH, Dakos V (2014) Early warning signals of ecological transitions: methods for spatial patterns. PLoS ONE 9(3):e2097
Kéfi S, Rietkerk M, Aiados CL, Pueyo Y, Papanastasis VP, ElAich A, de Ruiter PC (2007) Spatial vegetation patterns

and imminent desertification in Mediterranean arid systems. Nature 449:213–218
Kelly NM, Fonseca M, Whitfield P (2001) Predictive mapping for management and conservation of seagrass beds in North Carolina. Aquatic Conserv: Mar Freshw Ecosyst 11:437–451
Kenworthy WJ, Zieman JC, Thayer GW (1982) Evidence for the influence of seagrasses on the benthic nitrogen cycle in a coastal plain estuary near Beaufort, North Carolina (USA). Oecologia 54:152–158
King RS, Baker ME, Whigham DF, Weller DE, Jordan TE, Kazyak PF, Hurd MK (2005) Spatial considerations for linking watershed land cover to ecological indicators in streams. Ecol Appl 15:137–153
Kizaki S, Katori M (1999) Analysis of canopy-gap structure of forests by Ising-Gibbs states - equilibrium and scaling properties of real forests. J Phys Soc Jpn 68:2553–2560
Knutson TR, McBride JL, Chan J, Emanuel K, Holland G, Landsea C, Held I, Kossin JP, Srivastava AK, Sugi M (2010) Tropical cyclones and climate change. Nat Geosci 3:157–163
Koch EW (2001) Beyond light: physical, geological, and geochemical parameters as possible submerged aquatic vegetation habitat requirements. Estuaries 24:1–17
Koch EW, Ackerman JD, Verduin J, van Keulen M (2006) Fluid dynamics in seagrass ecology: from molecules to ecosystems. In: Larkum AWD, Orth RJ, Duarte M (eds) Seagrasses: biology, ecology and conservation. Springer, Dordrecht, pp 193–225
Lefcheck JS, Marion SR, Lombana AV, Orth RJ (2016) Faunal communities are invariant to fragmentation in experimental seagrass landscapes. PLoS ONE 11(5):e0156550
Livernois MC, Grabowski JH, Poray AK, Gouhier TC, Hughes AR, O'Brien KF, Yeager LA, Fodrie FJ (2017) Effects of habitat fragmentation on Zostera marina seed distribution. Aquat Bot 142:1–9
Malhotra A, Fonseca MS (2007) WEMo (wave exposure model): formulation, procedures and validation. NOAA Technical Memorandum NOS NCCOS 65. Beaufort, North Carolina, p 28
Marba N, Duarte CM (1995) Coupling of seagrass (*Cymodocea nodosa*) patch dynamics to subaqueous dune migration. J Ecol 83:381–389
Maxwell PS, Pitt KA, Olds AD, Rissik D, Connolly RM (2015) Identifying habitats at risk: simple models can reveal complex ecosystem dynamics. Ecol Appl 25:573–587
McGarigal K, Cushman SA, Ene E (2012) FRAGSTATS v4.2: spatial pattern analysis program for categorical maps. University of Massachusetts, Amherst. http://www.umass.edu/landeco/research/fragstats/fragstats.html
Micheli F, Bishop MJ, Peterson CH, Rivera J (2008) Alteration of seagrass species composition and function over two decades. Ecol Monogr 78:225–244
Mills KE, Fonseca MS (2003) Mortality and productivity of eelgrass Zostera marina under conditions of experimental burial with two sediment types. Mar Ecol Prog Ser 255:127–134
Moore KA, Jarvis JC (2008) Environmental factors affecting recent summer time eelgrass diebacks in the lower Chesapeake Bay: implications for long-term persistence. J Coast Res S 55:135–147
Moore KA, Shields EC, Parrish DB (2014) Impacts of varying estuarine temperature and light conditions on *Zostera marina* (eelgrass) and its interactions with *Ruppia maritima* (widgeongrass). Estuar Coasts 37(Suppl 1):S20–S30
Nordlund LM, Koch EW, Barbier EB, Creed JC (2016) Seagrass ecosystem services and their variability across genera and geographical regions. PLoS ONE 11(10):e0163091
Ooi JLS, Kendrick GA, Van Niel KP (2011) Effects of sediment burial on tropical rudereal seagrasses are moderated by clonal integration. Cont Shelf Res 31:1945–1954
Orth RJ, Carruthers TJB, Dennison WC, Duarte CM, Fourqurean JW, Heck KL, Hughes AR, Kendrick GA, Kenworthy WJ, Olyarnik Short FT, Waycott M, Williams SL (2006) A global crisis for seagrass ecosystems. Bioscience 56:987–996
Pascual M, Guichard F (2005) Criticality and disturbance in spatial ecological systems. Trends Ecol Evol 20:88–95
Patriquin DG (1975) 'Migration' of blowouts in seagrass beds at Barbados and Carriacou, West Indies and its ecological and geological applications. Aquat Bot 1:163–189
Perkins SE, Alexander LV, Nairn J (2012) Increasing frequency, intensity and duration of observed global heat waves and warm spells. Geophys Res Lett 39:L20714
Peterson CH, Fodrie J, Summerson HC, Powers SP (2001) Site-specific and density-dependent extinction of prey by schooling rays: generation of a population sink in top-quality habitat for bay scallops. Oecologia 129:349–356
Qian SS, Cuffney TF (2012) To threshold or not to threshold? That's the question. Ecol Indic 15:1–9
Qian SS, King RS, Richardson CJ (2003) Two statistical methods for the detection of environmental thresholds. Ecol Model 166:87–97
R Core Development Team (2017) R: A language and environment for statistical computing. R Foundation for Statistical Computing, Vienna, Austria. http://www.R-project.org/
Remmel TK, Csillag F (2003) When are two landscape pattern indices significantly different? J Geograph Syst 5:331–351
Reusch TBH (2002) Microsatellites reveal high population connectivity in eelgrass (*Zostera marina*) in two contrasting coastal areas. Limnol Oceanogr 47:78–85
Rietkerk M, Boerlijst M, van Langevelde F, HilleRisLambers R, van de Koppel J, Kumar L, Prins HHT, de Roos AM (2002) Self-organization of vegetation in arid systems. Am Nat 160:524–540
Rietkerk M, Dekker SC, de Ruiter PC, van de Koppel J (2004) Self-organized patchiness and catastrophic shifts in ecosystems. Science 305:1926–1929
Robbins BD, Bell SS (2000) Dynamics of a subtidal seagrass landscape: seasonal and annual change in relation to water depth. Ecology 81:1193–1205
Roberts DA, Adams JB, Smith MO (1993) Discriminating green vegetation, nonphotosynthetic vegetation and soils in AVIRIS data. Remote Sens Environ 44:255–269
Ruiz-Reynés D, Gomila D, Sintes T, Hernández-García E, Marbà N, Duarte CM (2017) Fairy circle landscapes under the sea. Sci Adv 3:e1603262
Samhouri JF, Levin PS, James CA, Kershner J, Williams G (2011) Using existing scientific capacity to set targets for ecosystem-based management: a Puget Sound case study. Mar Policy 35:508–518

SAS Institute Inc (2013) SAS 9.4 software package. SAS Institute, Cary, North Carolina

Sasaki T, Furukawa T, Iwasaki Y, Seto M, Mori AS (2015) Perspectives for ecosystem management based on ecosystem resilience and ecological thresholds against multiple and stochastic disturbances. Ecol Indic 57:395–408

Scanlon TM, Caylor KK, Levin SA, Rodriguez-Iturbe I (2007) Positive feedbacks promote power-law clustering of Kalahari vegetation. Nature 449:209–213

Scheffer M, Carpenter SR (2003) Catastrophic regime shifts in ecosystems: linking theory to observation. Trends Ecol Evol 18:648–656

Scheffer M, Hirota M, Holmgren M, Van Ness EH, Chapin FS (2012) Thresholds for boreal biome transitions. P Natl Acad Sci USA 109:21384–21389

Sheather SJ, Jones MC (1991) A reliable data-based bandwidth selection method for kernel density estimation. J R Stat Soc Ser B 53:683–690

Solé RV (2011) Phase Transitions. Princeton University Press, Princeton, p 240

Suchanek TH (1983) Control of seagrass communities and sediment distribution by *Callianassa* (Crustacea, Thalassinidea) bioturbation. J Mar Res 41:281–298

Suding KN, Hobbs RJ (2009) Threshold models in restoration and conservation: a developing framework. Trends Ecol Evol 24:271–279

Sumoski SE, Orth RJ (2012) Biotic dispersal in eelgrass *Zostera marina*. Mar Ecol Prog Ser 471:1–10

Thayer GW, Kenworthy WJ, Fonseca MS (1984) The ecology of eelgrassmeadows of the Atlantic Coast: a community profile. FWS/OBS-84/02. US Fish and Wildlife Service, Washington DC

Thomson JA, Burkholder DA, Heithaus MR, Fourqurean JW, Fraser MW, Statton J, Kendrick GA (2015) Extreme temperatures, foundation species, and abrupt ecosystem change: an example from an iconic seagrass ecosystem. Glob Change Biol 21:1463–1474

Toms JD, Lesperance ML (2003) Piecewise regression: a tool for identifying ecological thresholds. Ecology 84(8):2034–2041

Townsend EC, Fonseca MS (1998) Bioturbation as a potential mechanism influencing spatial heterogeneity of North Carolina seagrass beds. Mar Ecol Prog Ser 169:123–132

Turner MG, Gardner RH (2015) Landscape ecology in theory and practice. Springer-Verlag, New York

Uhrin AV, Townsend PA (2016) Improved seagrass classification using linear spectral unmixing. Estuar Coast Shelf Sci 171:11–22

Valentine JF, Heck KL Jr (1991) The role of sea urchin grazing in regulating subtropical seagrass meadows: evidence from field manipulations in the northern Gulf of Mexico. J Exp Mar Biol Ecol 154:215–230

van der Heide T, Bouma TJ, van Nes EH, van de Koppel J, Scheffer M, Roelofs JG, van Katwijk M, Smolders AJP (2010) Spatial self-organized patterning in seagrasses along a depth gradient of an intertidal ecosystem. Ecology 91(2):362–369

van der Heide T, Eklof JS, van Nes EH, van der Zee EM, Donadi S, Weerman EJ, Olff H, Eriksson BK (2012) Ecosystem engineering by seagrass interacts with grazing to shape an intertidal landscape. PLoS ONE 7(8):e42060

van der Heide T, van Nes EH, Geerling GW, Smolders AJP, Bouma TJ, van Katwijk MM (2007) Positive feedbacks in seagrass ecosystems: implications for success in conservation and restoration. Ecosystems 10:1311–1322

van der Heide T, van Nes EH, van Katwijk MM, Olff H, Smolders AJP (2011) Positive feedbacks in seagrass ecosystems – evidence from large-scale empirical data. PLoS ONE 6(1):e16504

Villarini G, Vecchi GA (2013) Projected increases in North Atlantic tropical cyclone intensity from CMIP5 models. J Climatol 26(10):3231–3240

Walker DI, Kendrick GA, McComb AJ (2006) Decline and recovery of seagrass ecosystems: the dynamics of change. In: Larkum AWD, Orth RJ, Duarte CM (eds) Seagrasses: biology, ecology and conservation. Springer, Dordrecht, pp 551–565

Warton DI, Hui FKC (2011) The arcsine is asinine: the analysis of proportions in ecology. Ecology 92:3–10

Waycott M, Duarte CM, Carruthers TJB, Orth RJ, Dennison WC, Olyarnik S, Calladine A, Fourqurean JW, Heck KL Jr, Hughes AR, Kendrick GA, Kenworthy WJ, Short FT, Williams SL (2009) Accelerating loss of seagrass across the globe threatens coastal ecosystems. Proc Natl Acad Sci USA 106:12377–12381

Weerman EJ, van Belzen J, Rietkerk M, Temmerman S, Kéfi S, Herman PMJ, van de Koppel J (2012) Changes in diatom patch-size distribution and degradation in a spatially self-organized intertidal mudflat ecosystem. Ecology 93:608–618

Williams AP, Hunt ER (2002) Estimation of leafy spurge cover from hyperspectral imagery using mixture tuned matched filtering. Remote Sens Environ 82:446–456